

# Efficiency Evaluation of Series Connected DC/DC Converters in On-Grid Solar PV System

<sup>1</sup>Slim ABID, <sup>2</sup>Ghazi Ben Hmida

<sup>1,2</sup>College of Engineering and Computer Science, Jazan University, Kingdom of Saudi Arabia

Authors E-mail: [smabid@jazanu.edu.sa](mailto:smabid@jazanu.edu.sa), [ghmida@jazanu.edu.sa](mailto:ghmida@jazanu.edu.sa)

**Abstract** - The grid-connected photovoltaic (PV) system is an important technology for renewable energy applications. It usually consists of three main stages: a PV module, a DC/DC converter and a DC/AC inverter. In these PV systems, Power Conditioning System should have high efficiency and low cost. In this paper, a classification of possible power converter topologies for PV panel integration is introduced. Out of different topologies of DC/DC converter, series connection of boost converters is more suitable converter for PV applications. In order to simulate the steady state efficiencies of the series connection of boost converters and the inverter non-ideal averaged model of these power converters is developed. Then the different elements and control of the (PV) system are implemented in Matlab/Simulink. Using loss analysis, the benefits and drawbacks of series connection of boost converters are shown. This analysis allowed the conception of an optimized architecture constituted by serialized power converters.

**Keywords:** grid-connected photovoltaic (PV) system, series connection, Non-ideal averaged Model of Power converters, Loss analysis.

## I. Introduction

Gulf states, including Saudi Arabia relies largely on oil and gas for the production of electrical energy. Since both of these sources will exhaust one day, it becomes necessary to look for new ways to obtain energy cheaply and safely. Nowadays world pays growing attention to the renewable energy sources. Due to its geographical location, the Kingdom of Saudi Arabia (KSA) has an abundant intensity of solar radiation and long duration of daylight hours. Hence, KSA is a good candidate for solar system applications. There is also a strategic national push to develop an energy efficiency and renewable technology and manufacturing base in an attempt to diversify the economy away from fossil fuels [1]. In this context, this research discusses the grid-connected photovoltaic (PV) system for residential buildings.

Today grid connected photovoltaic energy system is becoming more and more visible, with the increase of global electrical energy demand.

Based on the photovoltaic arrays power level, output voltage and applications, four configurations are widely used in photovoltaic grid-connected: centralized inverter system, the string inverter system, the multi-string inverter system and the module-integrated inverter system [2]–[4].

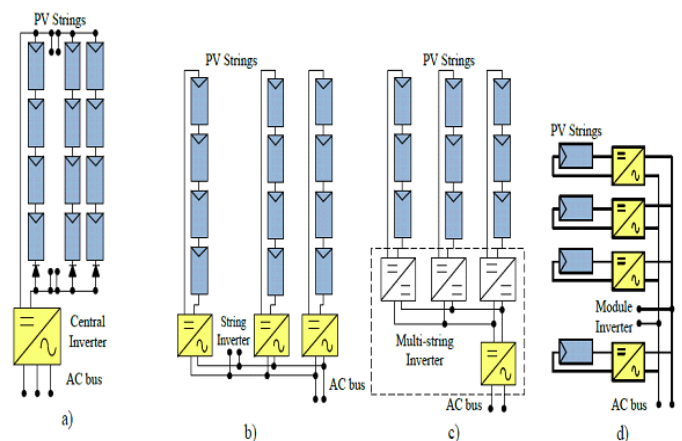


**Figure 1:** PV grid connected systems configurations a) Central Inverters; b) String Inverters c) Multi-String Inverters d) Module inverters [5]

In figure 1, the different topology of the photovoltaic is shown. The inverter could be a single stage inverter or dual stage inverter. Each topology has their advantages and disadvantages. In this work we have chosen the dual stage structure for its simplicity. The two-stage PV system is shown in figure 2.

A conventional two-stage grid-connected PV System is composed of PV panel, a DC/DC chopper and a DC/AC inverter that capably connected to the grid. This system is used for power generation in places or sites accessed by the electric utility grid. When the amount of energy generated by a PV system exceeds the owner's needs, excess energy is sent into the grid, turning the customer's electric meter backward. On the other hand, customer loads can be satisfied by the grid when power generated by the PV system is insufficient.

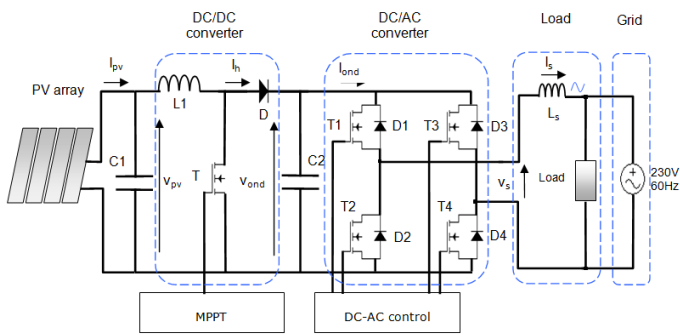


Figure 2: Dual-stage grid connected PV system with boost converter

The major role of DC/DC converter in photovoltaic system is to exploit more effectively the solar modules to extract maximum power from the pv system. The nonlinearity of the PV array (V-I characteristic) and the movement of the earth around the sun, further necessitate the application of maximum power point tracking (MPPT) to the system.

While the first stage is used to boost the PV array voltage and track the maximum solar power, the second stage inverts this dc power into high quality ac power.

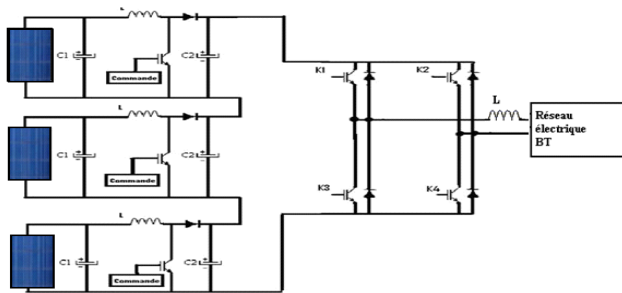


Figure 3: Electrical circuit of a discretized PV system with two stages (3 boost converters in series)

Due to relatively high costs and modest efficiency, the penetration of photovoltaic (PV) systems into the utility grid is low. Although Solar panel efficiency is obviously poor, the solar energy is a great opportunity for commercial buildings and residential.

To overcome this problem, the discretization of the PV panels, where each string of panels has its own adaptation stage seems an advantageous solution in order to increase the efficiency of the PV system [6]-[9]. Out of different topologies of DC/DC converter, series connection of boost converters is more suitable converter for PV applications. Figure 3 shows 3 cascaded DC/DC converters connected to a single central DC/AC inverter. Any DC/DC converter can be used for the cascaded converter. In this work Boost converters are used.

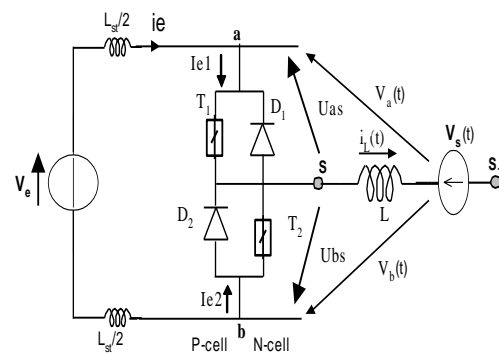
In order to simulate the steady state efficiencies of the series connection of boost converters and the inverter, non-

ideal averaged model of these power converters will be developed. We also proposed a model for photovoltaic cell. This model can work well under sudden change of environment temperature or solar radiation. The maximum power of the PV cell is tracked with an adjusted P&O MPPT algorithm based on the Boost DC/DC converter.

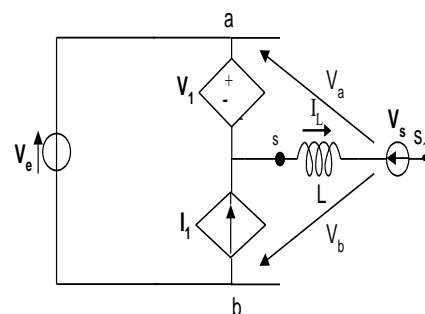
Using loss analysis, the benefits and drawbacks of series connection of boost converters will be shown. This analysis will allow the conception of an optimized architecture constituted by serialized power converters.

## II. The Non-Ideal Averaged Model of PWM Switch

Averaged circuit models for switching power converters is a simplified representation of the converter during switching time cycle that pictures the energy transformation without using explicitly any switching function. The method proceeds in a systematic fashion by determining appropriate averaged circuit elements that are consistent with the averaged circuit waveforms. Figure 4.a illustrates the studied PWM-switch structure, it has two basic switching cells (P-cell and N-cell). Each cell consists of one controlled switch and one diode. The Dc loop inductance is presented by an inductor  $L_{st}$  and the load is modeled by a voltage source ( $V_s$ ) in series with an inductor  $L$ .



(a)



(b)

Figure 4: (a) The PWM-switch, (b) The proposed equivalent circuit of the PWM-Switch averaged model

## 2.1 The Developed Averaged Model in Continuous Conduction Mode (CCM)

The developed averaged equivalent circuit model of the switching network of Figure 4.a is illustrated in Figure 4.b. This model is composed of controlled current source (I1) and controlled voltage source (V1). The switching semiconductor devices are the only nonlinear elements which are supposed to be responsible for the non linear behavior of the converter.

Considering  $T_s$  as the switching period of the controlled switches and  $(d)$  the duty ratio which is the ratio of the on-time value ( $T_{on}$ ) of the upper controlled switch (T1) and the switching period  $T_s$ .

The amplitudes of the two controlled sources are obtained by computing the time averaged values of the instantaneous terminal waveforms  $U_{as}(t)$  and  $i_{e2}(t)$  respectively over one cycle  $T_s$ .

In Figure (4.b), the current source ( $I_1$ ) and the voltage source ( $V_1$ ) are given by:

$$V_1 = \langle U_{as} \rangle$$

$$I_1 = \langle i_{e2} \rangle$$

For positive current,  $i_L(t)$ , Figure 5 shows the adopted switching characteristics of the controlled device  $T_1$  ( $U_{as}(t)$ ,  $i_{e1}(t)$ ) and the free-wheeling diodes  $D_2$  ( $U_{bs}(t)$ ,  $i_{e2}(t)$ ) during  $T_s$ .

$E_{g1}$  and  $E_{g2}$  are the driving signal of the controlled components  $T_1$  and  $T_2$ , respectively. We notice that Dc loop inductance, the reverse recovery phenomena and the dead time  $\delta$  between the two driving signals are taken into account.

We notice that the load current  $I_L$  is considered constant and equal to the averaged value of the real current  $i_L(t)$  in the load over the switching period  $T_s$ .

During devices turn-on and turn-off phases, the different voltage magnitude are given by

$$V_x = -(L_{st}(\frac{dI_F}{dt} + \frac{dI_R}{dt}) - V_d) \quad (1)$$

$$V_{RM} = -(V_e + L_{st} \frac{dI_R}{dt} - V_t) \quad (2)$$

$$V_{st} = L_{st} \frac{dI_F}{dt} \quad (3)$$

$$V_q = V_e + V_d - L_{st} \frac{dI_F}{dt} \quad (4)$$

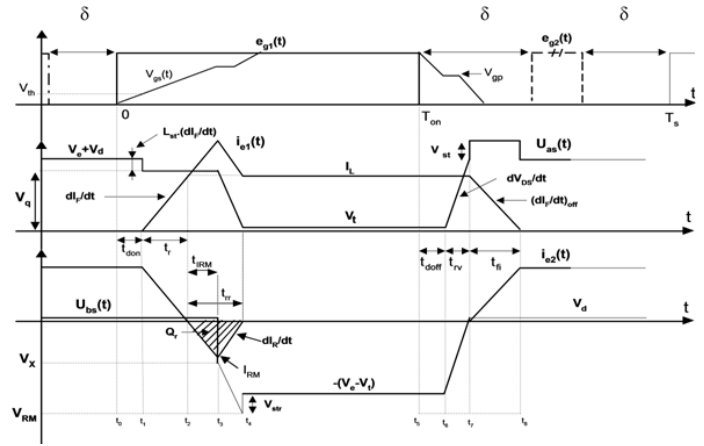


Figure 5: PWM-switch (upper Controlled device and lower diode) voltage and current waveforms ( $I_L > 0$ )

The parameter  $\delta$  is the dead-time fixed by the user to eliminate the simultaneous conduction of the two controlled devices of the bidirectional PWM-switch.

To eliminate the conduction of the two active devices at the same time, the following condition should be considered.

$$\delta > t_{doff} + t_{fi} + t_{rv} - t_{don} \quad (5)$$

The lower value of the on state time of the active device should be greater than the on transient switching time, so

$$(1-d)T_s - 2\delta > t_{don} + t_{rr} + t_r \quad (6)$$

The voltage source  $V_1$  expression is given by:

$$V_1 = V_{a1} \text{sign}(I_L) + V_{a2} \text{sign}(\bar{I}_L) \quad (7)$$

Where

$$\text{sign}(I_L) = \begin{cases} 1 & \text{if } I_L \geq 0 \\ 0 & \text{if } I_L < 0 \end{cases}$$

and

$$\text{sign}(\bar{I}_L) = \begin{cases} 0 & \text{if } I_L \geq 0 \\ 1 & \text{if } I_L < 0 \end{cases}$$

The averaged value of the  $U_{as}(t)$  voltage for continuous conduction mode (CCM) and  $I_L \geq 0$  is given by the following equation.

$$V_{a1} = \frac{V_e + V_d}{T_s} \left[ T_s - T_{on} - t_{doff} + t_{don} - \frac{t_{rv}}{2} \right] - \frac{V_t}{T_s} \left[ \frac{1}{2} (t_{rr} + t_{IRM} - t_{rv}) - T_{on} + t_{don} - t_{doff} + t_r \right] + \frac{V_{st}}{T_s} t_{fi} + \frac{V_b}{T_s} \left[ \frac{t_{rr} + t_{IRM}}{2} + t_r \right] \quad (8)$$

The controlled current source  $I_1$  expression is given by:

$$I_1 = I_{av1} \text{sign}(I_L) + I_{av2} \text{sign}(\bar{I}_L) \quad (9)$$

Where

$$I_{av1} = \frac{I_L}{T_s} \left[ T_s - T_{on} - t_{doff} - t_{rv} + t_{don} - \frac{(t_{fi} - t_r)}{2} \right] + I_{RM} \frac{t_{rr}}{2T_s} \quad (I_L \geq 0) \quad (10)$$

The output average current is deduced from the following state equation:

$$\frac{dI_L}{dt} = [V_a(t) - V_1] \frac{1}{L} \quad (11)$$

The voltage  $V_a(t)$  depends on  $V_s(t)$ ,  $V_e(t)$  and converter configuration.

### III. The Developed Averaged Model in Discontinuous Conduction Mode (DCM)

In DCM mode, the instantaneous current  $i_L(t)$  depends on circuit parameters and converter configuration. In fact, instantaneous voltage

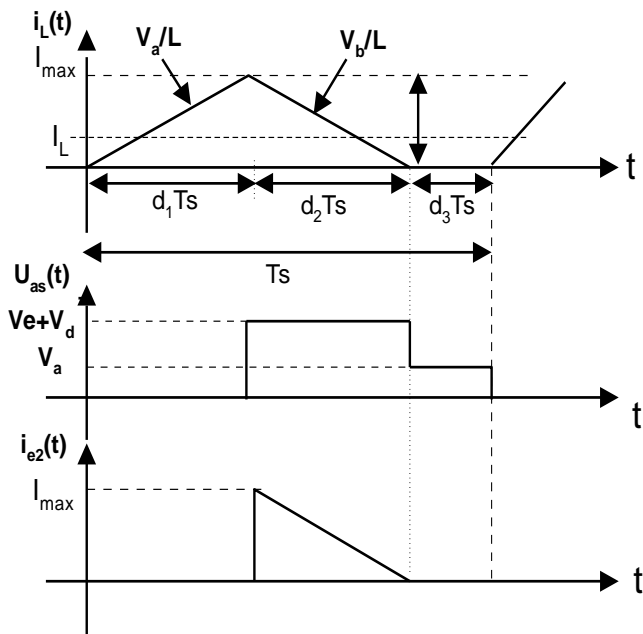


Figure 6: The DCM waveforms of the PWM-Switch in the case of positive inductor current

From figure 6, the averaged current  $I_L$  can be expressed by

$$I_L = \frac{I_{max}}{2} d_1 + \frac{I_{max}}{2} d_2 = \frac{(V_a - V_t) T_s d_1}{2L} (d_1 + d_2) \quad (12)$$

From equations 12,  $d_2$  can be expressed by

$$d_2 = \left( \frac{2L}{d_1 T_s} \frac{I_L}{(V_a - V_t)} - d_1 \right) \text{sign}(I_L) + \left( \frac{2L}{(1-d_1) T_s} \frac{I_L}{(V_b + V_t)} - (1-d_1) \right) \text{sign}(\bar{I}_L) \quad (13)$$

In discontinuous conduction mode, the averaged voltage value across the inductor  $L$  is equal to zero in each switching period  $T_s$ . In this condition, the controlled voltage source  $V_1$  is equal the average value ( $V_a$ ) of  $U_{as}(t)$ . From figure 6 we have

$$d_3 = 1 - d_1 - d_2$$

$$V_1 = V_a = d_2 (V_e + V_d) + V_a (1 - d_1 - d_2) + d_1 V_t$$

So (14)

$$V_1 = V_a = \frac{d_2}{d_1 + d_2} (V_e + V_d) + \frac{d_1}{d_1 + d_2} V_t \quad I_L \geq 0$$

In the case of a bidirectional PWM-Switch, the controlled voltage source can be written as:

$$V_{a1} = \frac{V_e + V_d}{T_s} \left[ T_s - T_{on} - t_{doff} + t_{don} - \frac{t_{rv}}{2} \right] - \frac{V_t}{T_s} \left[ \frac{1}{2} (t_{rr} + t_{IRM} - t_{rv}) - T_{on} + t_{don} - t_{doff} + t_r \right] + \frac{V_s}{T_s} t_{fi} + \frac{V_b}{T_s} \left[ \frac{t_{rr} + t_{IRM}}{2} + t_r \right] \quad (15)$$

Based on Figure 6, the controlled current source  $I_1$  can be expressed by the following equation

$$I_1 = \frac{I_{max}}{2} d_2 \quad (16)$$

Using equations 12 and 16, the current source  $I_1$  expression is given by

$$I_1 = \frac{d_2 I_L}{d_1 + d_2} \text{sign}(I_L) + \frac{(1-d_1) I_L}{(1-d_1) + d_2} \text{sign}(\bar{I}_L) \quad (17)$$

The proposed model can be made to automatically toggle from DCM to CCM when  $d_2$  is equals  $(1-d_1)$ .

In the case of DCM mode, the implemented algorithm calculates the  $V_a$  and  $V_b$  voltage from circuit voltage nodes value corresponding to the studied converter configuration. As an example, when the node  $s_1$  is connected to the node  $b$  in the circuit of Figure 4, the voltage  $V_b$  is equal to  $(-V_s)$  and the voltage  $V_a$  is equal to  $(V_e - V_s)$ .

#### IV. Modeling of PV Cell and MPPT Algorithm

##### 4.1 Modeling of PV cell

The PV cell is an electrical device, which directly converts the sunlight to electrical power. An equivalent circuit of the PV cell is depicted in figure 7. The PV cell is modeled as a current source in parallel with a diode.  $I_{ph}$ , the photovoltaic current is proportional to the ambient irradiance level and to the temperature of the panel. However no solar cell is ideal a series ( $R_s$ ) and parallel resistance ( $R_{sh}$ ) are commonly included in the circuit. Usually the value of  $R_{sh}$  is very large and that of  $R_s$  is very small, hence they may be neglected to simplify the analysis.

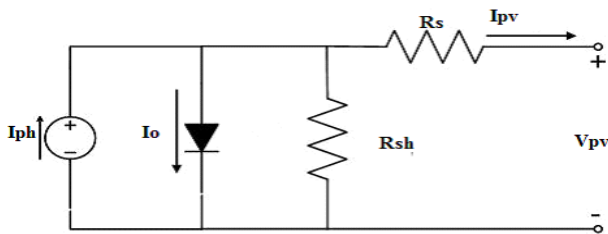


Figure 7: Equivalent Circuit of PV Cell

The (PV) mathematical model used to simplify our PV array is represented by the equations (18)-(21): [10]

Module Photo Current

$$I_{ph} = [I_{scR} + K_i (T - 298)] \times \frac{\lambda}{1000} \quad (18)$$

Module Reverse Saturation Current

$$I_{rs} = \frac{I_{scR}}{\exp\left(\frac{qV_{oc}}{NsAkT}\right) - 1} \quad (19)$$

Module Saturation Current

$$I_s = I_{rs} \left[\frac{T}{T_r}\right]^3 \exp\left[\left(q * \frac{E_{go}}{Bk}\right) \left(\frac{1}{T_r} - \frac{1}{T}\right)\right] \quad (20)$$

The Current Output of PV module is

$$I_{pv} = N_p \times I_{ph} - N_p \times I_o \left[\exp\left\{q * \frac{V_{pv} + I_{pv}R_s}{NsAkT}\right\} - 1\right] \quad (21)$$

Where:

- $V_{pv}$  is output voltage of a PV module (V)
- $I_{pv}$  is output current of a PV module (A)
- $T_r$  is the reference temperature = 298 K
- T is the module operating temperature in Kelvin
- $I_{ph}$  is the light generated current in a PV module (A)
- $I_o$  is the PV module saturation current (A)
- A = B is an ideality factor = 1.6

- k is Boltzmann constant =  $1.3805 \times 10^{-23}$  J/K
- q is Electron charge =  $1.6 \times 10^{-19}$  C
- $R_s$  is the series resistance of a PV module
- $I_{scR}$  is the PV module short-circuit current at  $25^\circ\text{C}$  and  $1000\text{W/m}^2 = 2.55\text{A}$
- $K_i$  is the short-circuit current temperature co-efficient at  $I_{scR} = 0.0017\text{A}/^\circ\text{C}$
- $E_{go}$  is the band gap for silicon =  $1.1\text{ eV}$
- $N_s$  is the number of cells connected in series
- $N_p$  is the number of cells connected in parallel
- $\lambda$  is the PV module illumination ( $\text{W/m}^2$ ) =  $1000\text{W/m}^2$

The model of photovoltaic solar panel implemented in MATLAB is based on the Solarex MSX60 module that the specifications are the following:

- Cell temperature  $T=25^\circ\text{C}$
- Open circuit voltage  $V_{oc}=21\text{V}$
- Short circuit current  $I_{sc}=3.74\text{A}$
- Current corresponding to the maximum power  $I_m=3.5\text{A}$
- Maximum Power  $P_m=59.9\text{W}$ .

The figure 8 shows the model of the pv panel implemented in simulink/matlab.

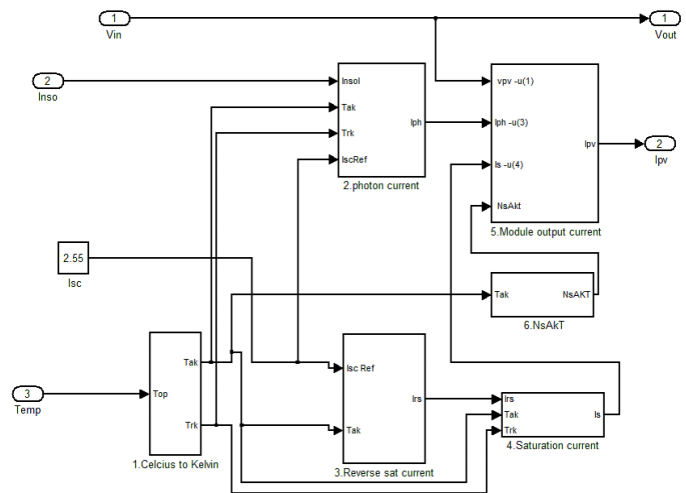


Figure 8: The model of the (PV) panel implemented in Matlab/simulink

In order to produce higher powers, the photovoltaic cells can be connected to create PV panels or modules. A series connection of cells increases the voltage of the generator, while the parallel connection increases its current. Today, in classical modules/arrays, series and parallel interconnections of PV cells are used to obtain the needed PV generator with the desired voltage and current characteristics.

Figure 9 shows the P-V Characteristic of (PV) array of 24 modules (4 strings of 6 series modules) obtained by simulation using Matlab/simulink. This configuration allows us to have a photovoltaic solar panel power equal to 1440W.

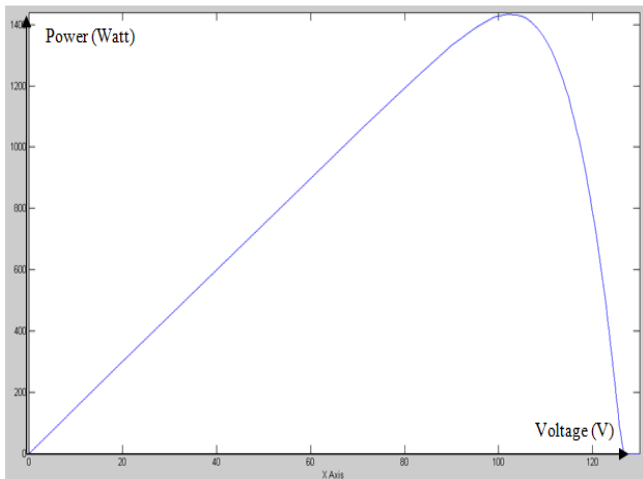


Figure 9: P-V Characteristic of (PV) array of 24 modules (4 strings of 6 series modules)

#### 4.2 PV control:

In the proposed PV energy conversion system, the perturbation and observation P&O algorithm is used in order to track maximum power point. This method widely used in MPPT because of their simple structure and high reliability [11]. The flow chart of the implemented algorithm is shown in Figure 10.

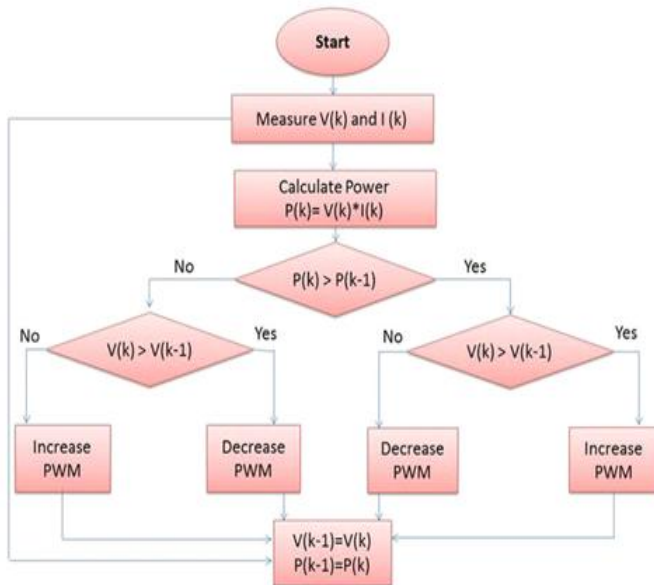


Figure 10: The flow chart of the implemented P&O algorithm

To extract the maximum power from the PV system, two controllers must be considered to control respectively the voltage ( $V_{pv}$ ) and the PV output current ( $I_{pv}$ ) which are the two state variables.

The first regulator imposes the optimal reference value of the current ( $I_{L-ref}$ ). This current is imposed to the second

controller of the DC/DC converter to adjust the voltage ( $V_{pv}$ ) to have the maximum power extraction.

The Fig.11 represented the block diagram of the PV strategy control.

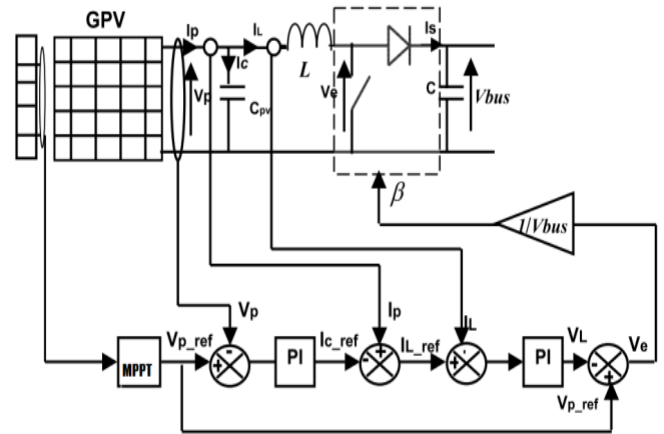


Figure 11: Block diagram of the PV control strategy

#### V. Efficiency Evaluation in Grid Connected Solar PV Generator

The figure 12 shows the complete blocks of PV generator implemented in MATLAB/simulink.

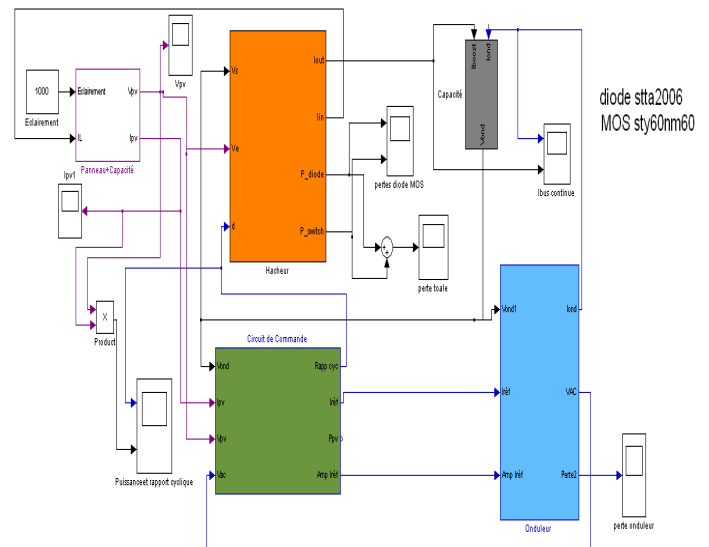


Figure 12: The complete blocks of PV generator implemented in MATLAB/simulink

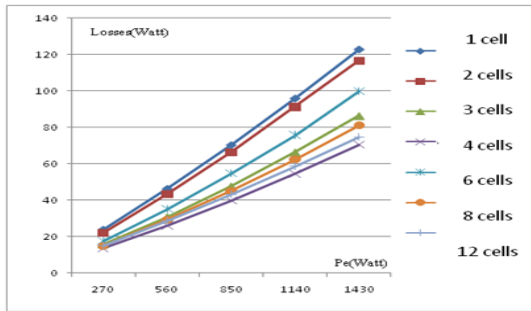
Due to the change of the static and dynamic characteristics according to each semiconductor manufacturer, we used two manufacturers for the MOSFET families to see the effect of these on the performance of the photovoltaic system.

Semiconductors used after the sizing of the electrical quantities (current and voltage) and according to the availability in the market, are summarized in the table 1.

Table 1

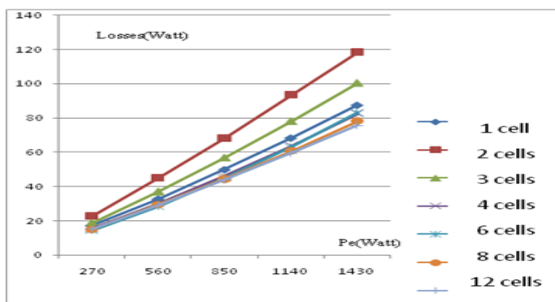
Number of the used boost converters	MOSFET used (ST Microelectronics)	Diodes used (ST Microelectronics)	MOSFET used (IR International Rectifier)
1	sty60nm60	stta2006	irfps43n50k
2	sty60nk30z	stth20r04	irfp4242pbf
3	stw52nk25z	stth2002	irfp4229pbf
4	stb40ns15	stth15020	irfb4615pbf
6	stp40nf10	stps20120d	irli2910
8	std45nf75	stps15h100cb	irfu2407
12	std35nf06l	stps1045	irfsl3806pbf

Also, we implemented all the structures proposed in MATLAB. It should be noted we did 70 simulations. For all configurations mentioned above (from 1 to 12 switching cells or boost converter in series) total losses in the PV system (Boost converter and the inverter) were evaluated according to the illumination. The evolutions of the waveforms of these losses for the different configurations are given in the diagram in Figure 13.a and Figure 13.b:



semiconducteurs STMicroelectronics

(a)



semiconducteurs International Rectifier

(b)

Figure 13: Evolution of total losses based on the input power, (a) semiconductors STMicroelectronics, (b) semiconductors International Rectifier

The following two figures show that the difference between the configuration with a single cell and 12 cells is considerable in terms of efficiency. Indeed, if we take the example of 4 cells we note that: for the STMicroelectronics devices losses represent 5% of the input power ( $P_e=1430W$ ).

## VI. Conclusion

Solar energy now present high costs, but progress is fast and the search is active. In this context, we described the various possible combinations of power converters for creating usable power modules for photovoltaic domestic applications. We also proposed a modified engineering model for photovoltaic cell. This model can work well under sudden change of environment temperature or solar radiation. The maximum power of the PV cell is tracked with an adjusted P&O MPPT algorithm based on Boost DC/DC converter. Also, we have developed an advanced PWM-Switch model operating in CCM and DCM modes. Contrarily to the classical averaged model, the proposed model takes into account the devices non linearity (on state voltage and switching characteristics), the circuit stray inductance and the driving signals nonlinearity (dead times).

The whole photovoltaic grid-connected system is simulated in MATLAB/Simulink. The results of simulation showed that the subdivision of the input power Boost converters dedicated to photovoltaic applications seems an advantageous solution in order to optimize and increase in solar power generation but the question arises today is the energy gain provided could cover the costs of such topology?

## REFERENCES

- [1] Y. Alyousef and M. Abu-ebid (2012). Energy Efficiency Initiatives for Saudi Arabia on Supply and Demand Sides, Energy Efficiency - A Bridge to Low Carbon Economy, Dr. Zoran Morvaj (Ed.), ISBN: 978-953-51-0340-0, InTech, Available from: <http://www.intechopen.com/books/energy-efficiency-a-bridge-to-low-carboneconomy/energy-efficiency-initiatives-for-saudi-arabia-on-supply-and-demand-sides>
- [2] Matthias Kasper, Dominik Bortis, Thomas Friedli and Johann W. Kolar Aalborg "Classification and Comparative Evaluation of PV Panel Integrated DC-DC Converter Concepts" University, Denmark, 2012 15th International Power Electronics and Motion Control Conference, EPE-PEMC 2012 ECCE Europe, Novi Sad, Serbia.
- [3] Xiangdong Zong. A Single Phase Grid Connected DC/AC Inverter with Reactive Power Control for Residential PV Application. Master's thesis,

- Department of Electrical and Computer Engineering University of Toronto, 2011.
- [4] Satheesh Kumar D. Ramya N.D. Indira R., R.Ashok “Design and Analysis of Single Phase Grid Connected Inverter » International Journal of Innovative Research in Computer and Communication Engineering Vol. 3, Issue 2, February 2015.
- [5] Vlad Alexandru Muresan. Control of Grid Connected PV Systems with Grid Support Functions. Master’s thesis, Department of Energy Technology - Pontoppidanstræde 101, Aalborg University, Denmark, 2012.
- [6] Merin George, Prasitha Prakash, Shilpa George, Susan Eldo, Annai Raina “Cascaded Boost Converter for PV Applications” INTERNATIONAL JOURNAL OF INNOVATIVE RESEARCH IN ELECTRICAL, ELECTRONICS, INSTRUMENTATION AND CONTROL ENGINEERING Vol. 2, Issue 4, April 2014.
- [7] Ganga. M “Power Optimization Strategy of a Cascaded Dc/Dc Converter Topologies for Grid Connected Photo Voltaic System” International Journal of Innovative Research in Science, Engineering and Technology Volume 3, Special Issue 3, March 2014.
- [8] Vázquez-Guzmán Gerardo « High Efficiency Single-Phase Transformer-less Inverter for Photovoltaic Applications » Ingeniería Investigación y Tecnología, volumen XVI (número 2), abril-junio 2015: 173-184.
- [9] Yuxin Liang “Parallel Coordination Control of Multi-Port DC-DC Converter for Stand-Alone Photovoltaic-Energy Storage Systems” CPSS Transactions on Power Electronics and Applications September 2020 5(3):235-241.
- [10] Mr. Pandiarajan Natarajan « Performance Improvement of PV Module at Higher Temperature Operation » IRACST – Engineering Science and Technology: An International Journal (ESTIJ), ISSN: 2250-3498, Vol.2, No. 5, October 2012.
- [11] I.Vedasangamithra, N.Selvarani “Design and analysis of various MPPT algorithms for CHBMLI” International Journal of Advanced Research in Electrical, Electronics and Instrumentation Engineering Vol. 3, Issue 2, February 2014.
- [12] E. Benkhelil and A. Gherbi “Modeling and simulation of grid-connected photovoltaic generation system” Revue des Energies Renouvelables SIENR’12 Ghardaïa (2012) 295 – 306.

**Citation of this Article:**

Slim ABID, & Ghazi Ben Hmida. (2024). Efficiency Evaluation of Series Connected DC/DC Converters in On-Grid Solar PV System. *International Research Journal of Innovations in Engineering and Technology - IRJIET*, 8(6), 63-70. Article DOI <https://doi.org/10.47001/IRJIET/2024.806008>

\*\*\*\*\*